Inorganic Chemistry

Article

pubs.acs.org/IC

Synthesis of a NbO Type Homochiral Cu(II) Metal−Organic Framework: Ferroelectric Behavior and Heterogeneous Catalysis of Three-Component Coupling and Pechmann Reactions

Anoop K. Gupta,[†] Dinesh De,[†] Rajesh Katoch,[‡] Ashish Garg,[‡] and Parimal K. Bharadwaj*,[†]

[†]Department of Chemistry, Indian Institute of Technology Kanpur, Kanpur, UP 208016, India

[‡]Department of Materials Science and Engineering, Indian Institute of Technology Kanpur, Kanpur, UP 208016, India

Supporting Information

ABSTRACT: A chiral tetracarboxylic acid ligand, $\mathbf{H_4L}$, incorporating the (*S*)-(+)-2-methylpiperazine moiety in its middle, solvothermally forms a homochiral Cu(II) framework, $\{[Cu_2(\mathbf{L})(H_2O)_2]\cdot(4DMF)(4H_2O)\}_n$ (**LCu**). It forms a non-interpenetrated structure consisting of $[Cu_2(COO)_4]$ paddle-wheel secondary bonding units (SBUs) with *NbO* topology. Interestingly, the framework **LCu** exhibits excellent ferroelectric properties. It shows a remnant polarization (Pr) of ∼3.5 μC cm^{-2} and a coercive field (E_c) of ∼12 kV cm^{-1} with a distinct electric hysteresis loop. Dielectric studies of **LCu** reveal almost frequency-independent behavior with a dielectric constant (ε_r) of ∼42 and a low dielectric loss (tan δ) of ∼0.04 up to 10^6 Hz, for potential use in high-frequency applications. In addition, activated framework **LCu′** having uncoordinated metal sites acts as an efficient heterogeneous catalyst in the three-component coupling of amines, aldehydes, and alkynes, as well as in Pechmann reactions of phenols with β-ketoesters.

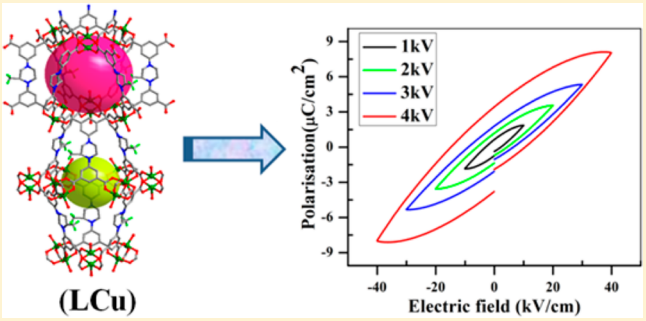

INTRODUCTION

Metal−organic frameworks (MOFs), especially when they form highly porous structures, exhibit fascinating properties arising from the organic−inorganic ensembles[1] that have already resulted in a wide range of applications. Some of the important applications of these materials that are vigorously pursued include gas storage and separation, heterogeneous catalysis, enantioselective separation, sensing through luminescence, ferroelectricity, magnetism, etc.[2−7] Interestingly, integration of these applications in a suitably designed multifunctional MOF[8] remains a challenge that can be addressed via selection of the metal and/or functional organic linkers.[9] This deliberately tunes the optical, ferroelectric, magnetic, catalytic, and adsorption properties of MOFs.[3,10,11]

Ferroelectric materials have important scientific and technological applications in the fabrication of capacitors, resonators, communication systems, data storage devices, etc.[12−15] In particular, materials possessing high dielectricity are important in dielectric resonators and filters for microwave communication systems.[16,17] In recent years, a great deal of attention has been focused on developing typical ferroelectric/dielectric materials. These kinds of ferroelectric/dielectric materials are mostly traditional inorganic materials, such as ceramics, inorganic salts, and their derivatives.[18] The synthesis of these materials is still challenging because it demands extreme reaction conditions such as the very high temperatures required for crystallization and sintering.[19] Thus, the design and synthesis of new ferroelectric and dielectric materials have attracted an enormous amount of interest from the scientific community. The facile synthesis of MOFs at relatively low temperatures (<200 °C) makes them interesting materials for ferroelectric purposes.[20−22] However, development of MOF-based ferroelectric materials demands that the compound have chiral centers for crystallization in noncentrosymmetric space groups.[23−25] This can be obtained by adopting the strategies such as the use of chiral ligands, chiral templates and counter cations, and auxiliary ligands. Huang et al. reported an (*S*)-1,4-diallyl-2-methylpiperazine (DAMP)-based novel homochiral three-dimensional (3D) framework that displays ferroelectric behavior.[19] Previously, our group reported an (*S*)-(+)-2-methylpiperazine-based semiflexible homochiral ligand in constructing a Cd(II) ion-containing 3D coordination polymer that exhibited interesting ferroelectric and dielectric properties.[26]

Additionally, MOFs with a large surface area and coordinatively unsaturated metal centers (UMCs) have provided opportunities for applications in heterogeneous catalysis.[27,28] Here, the UMC can act as a Lewis acid center for various acid-catalyzed organic reactions.[29] MOFs as heterogeneous catalysts have attracted a huge amount of interest from both industry and academia.[30−32] Among

Received: February 7, 2017

DOI: 10.1021/acs.inorgchem.7b00342
Inorg. Chem. XXXX, XXX, XXX−XXX

different types of MOFs, copper-based frameworks have shown catalytic properties for numerous organic transformations.[33−37]

In this context, we designed and synthesized a chiral tetracarboxylic acid ligand, incorporating dicarboxylate units at the termini, i.e., 5,5′-[(*S*)-(+)-2-methylpiperazine-1,4-diyl]-diisophthalic acid [H_4**L** (Scheme 1)]. This ligand solvothermally forms a non-interpenetrated MOF, **LCu**, containing paddle-wheel SBUs (Figure 1a), which is based on the following rationale. (i) Terminal isophthalate moieties prefer paddle-wheel SBUs, and four carboxylic groups in H_4**L** are likely to form a porous system.[38] (ii) The incorporated (*S*)-(+)-2-methylpiperazine moiety will ensure crystallization in a noncentrosymmetric space group.

Scheme 1. Schematic Diagram of Chiral Ligand H_4L

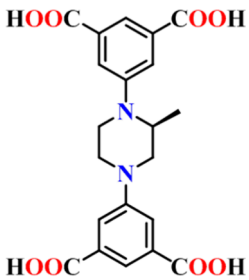

(H_4L)

We show that **LCu** exhibits interesting ferroelectric properties with a hysteresis loop. The guest-free framework with UMCs (**LCu′**) showed excellent heterogeneous catalytic activity in a one-pot synthesis of imidazopyridines through three-component coupling reactions of amines, aldehydes, and alkynes as well as the Pechmann condensation reactions to synthesize coumarin derivatives.

EXPERIMENTAL SECTION

Materials. Reagent grade chemicals (*S*)-(+)-2-methylpiperazine, dimethyl-5-bromoisophthalate (97%), (±)-BINAP (97%), $Pd(OAc)_2$ (98%), and $Cu(NO_3)_2{\cdot}3H_2O$ (99%) were obtained from Sigma-Aldrich. These chemicals were used as received. All other chemicals and solvents were purchased from S. D. Fine Chemicals and were freshly purified prior to use.

Physical Measurements. The details of physicochemical characterization and single-crystal X-ray investigation are given in the Supporting Information.

Synthetic Methodology. The tetracarboxylic acid ligand 5,5′-[(*S*)-(+)-2-methylpiperazine-1,4-diyl]diisophthalic acid, H_4**L**, was synthesized by following a reported procedure[39] as illustrated in Scheme 2.

Synthesis of Tetramethyl 5,5′-[(*S*)-(+)-2-Methylpiperazine-1,4-diyl]diisophthalate. A mixture of (*S*)-(+)-2-methylpiperazine (500 mg, 5 mmol) and dimethyl 5-bromoisophthalate (2.73 g, 10.00 mmol) in toluene (40 mL) was combined with cesium carbonate (3.91 g, 12.00 mmol), (±)-BINAP (62 mg, 0.1 mmol), and palladium acetate (17 mg, 0.075 mmol). The mixture was vigorously stirred at 110 °C for 2 days. After this, the reaction mixture was cooled to room temperature and the solvent was evaporated under reduced pressure; water (150 mL) was added, and then the compound was extracted with ethyl acetate. The collected organic phases were further shaken with brine and passed through anhydrous sodium sulfate. After evaporation to dryness, the crude product was obtained as a yellow solid that was purified by column chromatography using silica gel (200 mesh). Elution with 30% ethyl acetate in *n*-hexane gave 5,5′-[(*S*)-(+)-2-methylpiperazine-1,4-diyl]diisophthalate as a pale yellow crys-

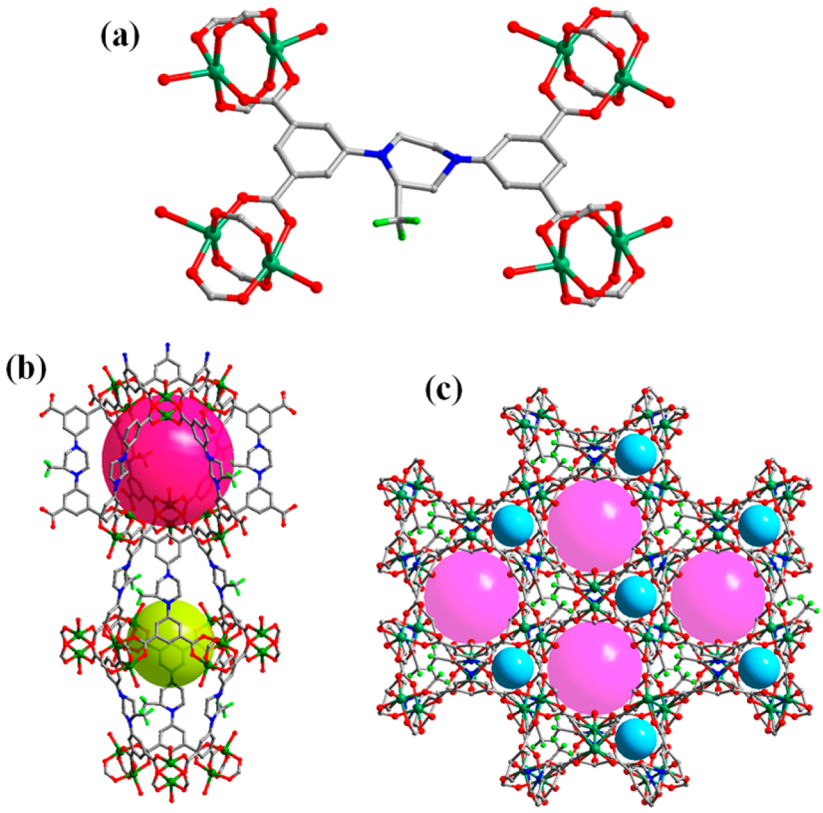

Figure 1. (a) Coordination environment around the Cu^{2+} ions in **LCu**. (b) View of the cages. (c) Perspective view of the 3D packing of **LCu** along the crystallographic *c*-axis showing two types of pores.

DOI: 10.1021/acs.inorgchem.7b00342
Inorg. Chem. XXXX, XXX, XXX−XXX

Scheme 2. Synthesis of Ligand H_4L

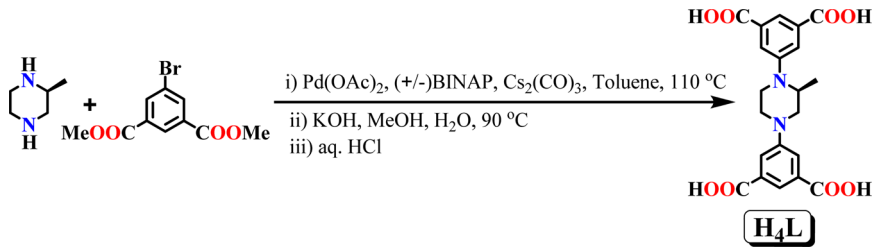

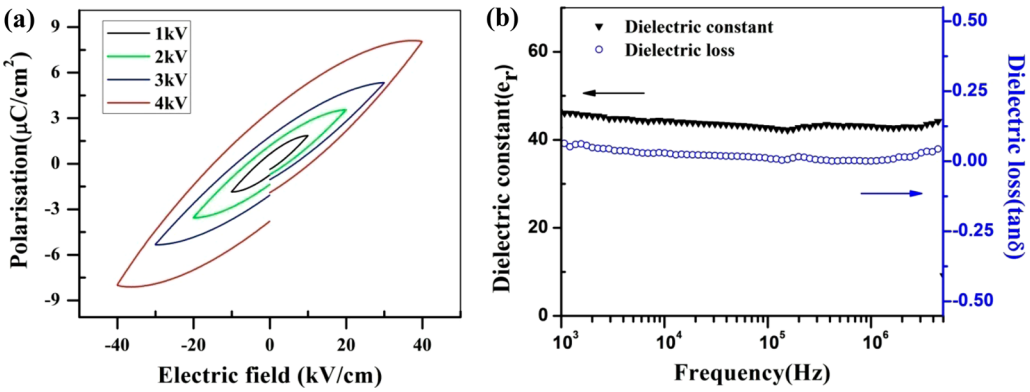

Figure 2. (a) View showing the plot of polarization (P_r) vs applied electric field (E_c). (b) Frequency dependence of the dielectric constant and dielectric loss of **LCu** at room temperature.

talline powder [600 mg yield, 25% based on (*S*)-(+)-2-methylpiperazine]: ^{1}H NMR [500 MHz, $CDCl_3$, 25 °C, $Si(CH_3)_4$] δ 8.15 (s, 2H, Ar-H), 7.77 (s, 4H, Ar-H), 4.20−4.18 (m, 1H, -CH_2-), 3.94 (s, 12H, -COOMe), 3.76−3.74 (m, 1H, -CH_2-), 3.58−3.51 (m, 2H, -CH_2-), 3.37−3.30 (m, 2H, -CH_2-), 3.15−3.11 (m, 1H, CH), 1.19 (d, J = 6.30 Hz, 3H, -Me); ^{13}C NMR [125 MHz, $CDCl_3$, 25 °C, $Si(CH_3)_4$] δ 13.4 (-CH_3), 43.3 (-CH_2-), 48.6 (-CH_2-), 51.4 (-OCH_3), 52.5 (-CH_2-), 54.3 (CH), 120.9 (Ar-C), 131.6 (Ar-C), 132.4 (Ar-C), 150.0 (Ar-C), 166.8 (-CO-); ESI-MS m/z 485.1925 (100%) (calcd for $[M + H]^+$ m/z 485.1924). Anal. Calcd (%) for $C_{25}H_{28}N_2O_8$: C, 61.97; H, 5.20; N, 5.78. Found: C, 62.42; H, 5.48; N, 5.54.

Synthesis of 5,5′-[(*S*)-(+)-2-Methylpiperazine-1,4-diyl]-diisophthalic Acid (H_4L). The tetraester (500 mg, 1.03 mmol) and KOH (210 mg, 3.75 mmol) were mixed in methanol (40 mL) and water (20 mL). The reaction mixture was refluxed for 24 h. The solvent was evaporated under reduced pressure, and water was added to the mixture. The aqueous solution was acidified with concentrated HCl to pH ∼5 whereupon the product precipitated as a light yellow solid. It was collected by filtration. The solid was washed with water and dried in vacuo to obtain **H_4L** (398 mg yield, 90%): mp >300 °C; ^{1}H NMR [500 MHz, d_6-DMSO, 25 °C, $Si(CH_3)_4$] δ 13.12 (broad, 4H, -COOH), 7.89−7.86 (m, 2H, Ar-H), 7.66−7.63 (m, 4H, Ar-H), 4.22−4.21 (m, 1H, -CH_2-), 3.78−3.75 (m, 1H, -CH_2-), 3.64−3.62 (m, 1H, -CH_2-), 3.55−3.52 (m, 1H, -CH_2-), 3.22−3.17 (m, 2H, -CH_2-), 3.01−2.96 (m, 1H, CH), 1.08 (d, J = 5.7 Hz, 3H, -Me); ^{13}C NMR [125 MHz, d_6-DMSO, 25 °C, $Si(CH_3)_4$] δ 13.2 (-CH_3), 42.3 (-CH_2-), 48.1 (-CH_2-), 50.7 (-CH_2-), 53.58 (CH), 119.8 (Ar-C), 121.5 (Ar-C), 132.6 (Ar-C), 150.1 (Ar-C), 151.9 (Ar-C), 167.5 (-COOH); ESI-MS m/z 427.1151 (100%) (calcd for $[M - H]^-$ m/z 427.1141). Anal. Calcd (%) for $C_{21}H_{20}N_2O_8$: C, 58.87; H, 4.70; N, 6.54. Found: C, 59.15; H, 4.53; N, 6.69.

Synthesis of $\{[Cu_2(L)(H_2O)_2]\cdot(4DMF)(4H_2O)\}_n$ (LCu). $Cu(NO_3)_2\cdot 3H_2O$ (35 mg, 0.15 mmol), **H_4L** (20 mg, 0.05 mmol), and concentrated HCl (2 drops) were dissolved in a mixture of DMF (2 mL) and H_2O (1 mL). The solution was taken in a Teflon-lined stainless steel autoclave. The autoclave was heated under autogenous pressure to 90 °C for 48 h and then allowed to cool to room temperature at a rate of 10 °C/h. Blue-colored block-shaped crystals of **LCu** were collected by filtration: yield 49%; FT-IR (KBr pellets) 3430 (br), 2930 (m), 1660 (s), 1585 (s), 1417 (s), 1384 (s), 1255 (m), 1226 (m), 1163 (m), 1100 (s), 1017 (s), 776 (s), 729 (s) cm^{-1}. Anal. Calcd (%) for $C_{33}H_{56}N_6O_{18}Cu_2$: C, 41.63; H, 5.93; N, 8.83. Found: C, 42.19; H, 5.68; N, 8.36.

■ RESULTS AND DISCUSSION

Ligand **H_4L** reacts with $Cu(NO_3)_2\cdot 3H_2O$ (1:4 molar ratio) under solvothermal conditions to form $\{[Cu_2(\mathbf{L})(H_2O)]\cdot(4DMF)(4H_2O)\}_n$ (**LCu**). X-ray structural analysis revealed that **LCu** was a non-interpenetrated 3D MOF and isoreticular to the known NOTT-101 structure.[40] The asymmetric unit contained one $\mathbf{L}^{4-}$ ligand and two Cu(II) ions with one coordinated water molecule on each Cu(II) ion (Figure 1a). In addition, lattice DMF and water molecules were also present. The Cu(II) ions formed a $[Cu_2(COO)_4(H_2O)_2]$ paddle-wheel SBU in which each metal ion showed square-pyramidal coordination geometry with equatorial ligation from four bridging carboxylates and one water molecule bound axially (Figure 1a). The methyl group on the piperazine ring and the piperazine moiety showed disorder because of rotational freedom.

In the paddle-wheel structure, the Cu···Cu separation was 2.6453(11) Å. The equatorial Cu−O distances spanned the range of 1.915(8)−2.000(9) Å, which suggested strong metal−carboxylate bonding. The axially bound water molecules showed the Cu1−OW1 and Cu2−OW2 distances to be 2.049(6) and 2.208(7) Å, respectively. All these bond lengths were comparable to those found in the literature for similar structures.[41]

These paddle-wheel SBUs were bridged by the carboxylates of $\mathbf{L}^{4-}$ showing a *NbO* topology with the point symbol $6^4.8^2$. The framework showed large cages (Figure 1b) with a dimension of 13.88 Å (distance refers to the Cu-to-Cu connection) occupied by DMF and water molecules. There are two more channels of different sizes along the crystallo-

DOI: 10.1021/acs.inorgchem.7b00342
Inorg. Chem. XXXX, XXX, XXX−XXX

Table 1. LCu′-Catalyzed Synthesis of Imidazopyridine Compounds through a TCC and 5-Exo-dig Cyclization Reaction[a]

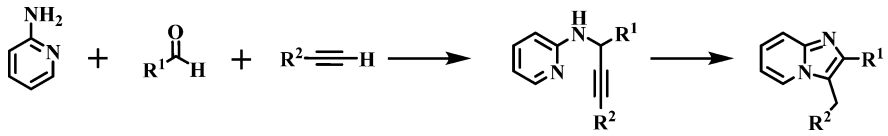

Entry	Catalyst	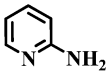	R^1COH	$R^2C{\equiv}CH$	Yield (%)[b]
1	L_{Cu}'	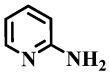	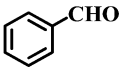	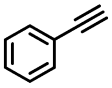	89
2	L_{Cu}'	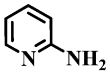	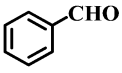	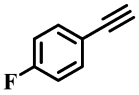	86
3	L_{Cu}'	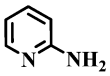	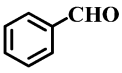	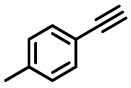	81
4	L_{Cu}'	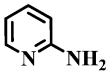	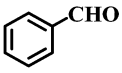	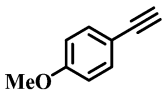	77
5	L_{Cu}'	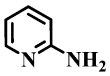	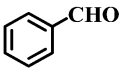	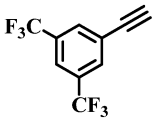	73
6	$Cu(OAc)_2{\cdot}H_2O$	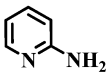	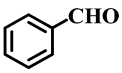	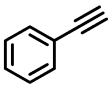	38
7	No Catalyst	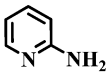	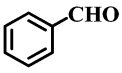	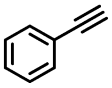	<3

[a]Reaction conditions: 2-aminopyridines (1.1 mmol), benzaldehydes (1.2 mmol), aryl alkynes (1 mmol), in toluene (1 mL), catalyst **LCu′** (10 wt %), sealed tube at 120 °C for 30 h under N_2. [b]Yield of the isolated product.

graphic *c*-axis (Figure 1c). The guest solvent molecules were highly disordered; hence, squeezed refinement was performed. The $4DMF/4H_2O$ solvent composition was calculated on the basis of the thermogravimetric weight loss analysis (TGA), IR spectra, and elemental analysis. The values obtained were in good agreement with the PLATON-calculated solvent-accessible void volume. The calculated solvent-accessible void volume was found to be 67% of the unit cell volume.

Ferroelectric and Dielectric Properties. As the X-ray studies revealed that the sample crystallized in the *R*3 space group associated with point group C_3, it lacked an inversion symmetry, which in turn satisfied the necessary condition for the development of ferroelectricity. Ferroelectricity arises as a result of uncompensated electric dipole moments due to the lack of inversion symmetry and manifests itself by the presence of spontaneous polarization. This polarization in turn can be switched by changing the applied electric field. Thus, to understand the macroscopic ferroelectric behavior, plots of polarization (P) versus applied field (E) at different applied field strengths are shown in Figure 2a. It was evident from the plots that the sample showed a well-defined ferroelectric response until the highest applied electric field was reached. The saturation polarization (P_s) was ~8 μC cm^{-2} at an applied electric field strength of 40 kV cm^{-1}. The value of remnant polarization ($2P_r$) was ~3.5 μC cm^{-2} with a coercive field (E_c) of ~12 kV cm^{-1}. In the study presented here, the value of saturation polarization (P_s) was notably larger than that of other ferroelectrics like KDP[17] (5.0 μC cm^{-2}) and several ferroelectric MOFs.[18,26,42] Recently, there has been a huge amount of interest in developing high-*k* and low-loss gate dielectrics to replace SiO_2 because of the high leakage currents encountered at the submicrometer thicknesses required for large scale integration. Therefore, we studied the dielectric behavior with respect to the change in frequency as shown in Figure 2b. The real dielectric constant value ($\varepsilon_r \sim 42$) of the sample remained fairly constant within the frequency range of 10^3–10^6 Hz. Similarly, it showed a low dielectric loss value (tan $\delta \sim 0.04$) over the entire frequency range investigated. However, both dielectric constant and dielectric loss increased abruptly at frequencies above 5 MHz, which could be caused by dipolar relaxation. The frequency-independent variation of dielectric behavior indicated that the dielectric response was free from interfacial polarization, and the dipolar polarization mechanism made the major contribution. A fairly high value of the dielectric constant with a low dielectric loss and concomitant well-saturated ferroelectric hysteresis loops further confirmed the intrinsic nature of ferroelectricity in the sample. These values are significant as most MOFs show ferroelectricity

DOI: 10.1021/acs.inorgchem.7b00342
Inorg. Chem. XXXX, XXX, XXX−XXX

Table 2. Substrate Screen for the Pechmann Condensation Reactions Catalyzed by LCu′[a]

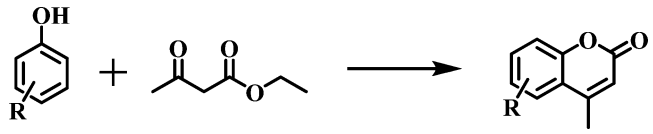

Entry	Catalyst	Substrate	Product	Yield (%)[b]
1	L_{Cu}'	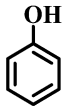	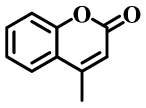	79
2	L_{Cu}'	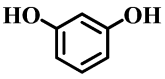	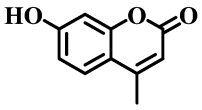	<2
3	L_{Cu}'	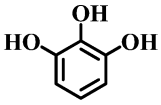	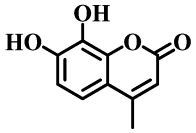	Trace
4	L_{Cu}'	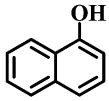	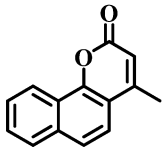	92
5	L_{Cu}'	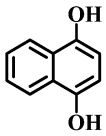	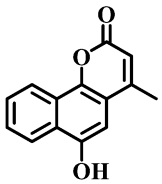	67
6	$Cu(OAc)_2 \cdot H_2O$	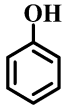	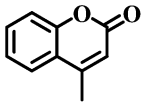	20
7	No Catalyst	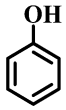	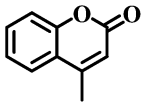	No Reaction

[a]Reaction conditions: phenolic compounds (2.1 mmol), ethyl acetoacetate (2.5 mmol), **LCu′** (10 wt %) as the catalyst, 130 °C for 24 h. [b]Yield of the isolated product.

below room temperature[43−47] or are only weakly ferroelectric near room temperature.[48−52]

The ferroelectric properties of this compound were on par with the one of the most extensively studied organic ferroelectrics, PVDF, i.e., polyvinylidene fluoride, and its composite ferroelectrics.[53−55] Additionally, **LCu** was found to be stable up to ∼250 °C (T_c ∼ 180 °C) comparing PVDF with a melting point of ∼170 °C (T_c ∼ 140 °C).[56] The fairly stable dielectric constant (ε_r ∼ 42) and low dielectric loss (tan δ ∼ 0.04) in the frequency range of this material are desirable and comparable with most literature reports from the point of view of large scale integration scalability[53] and energy storage applications.[57]

One-Pot Synthesis of Imidazopyridine Derivatives through a Three-Component Coupling and 5-Exo-dig Cyclization Reactions. A large pore volume and axially bound water molecules are two key aspects of the structure of **LCu**. Because upon heat treatment, **LCu** can be activated to have **LCu′** where all the guest solvent molecules as well as the metal-bound aqua ligand are removed without breakdown of the framework, it was probed as a heterogeneous catalyst in different organic transformation reactions. Herein, we establish a proficient synthesis of imidazopyridines by **LCu′**-catalyzed three-component coupling (TCC) reaction of 2-aminopyridines with benzaldehydes and aromatic alkynes to afford different imidazopyridine derivatives. Over the years, N-heteroaromatic compounds have been regarded as being very important for the synthesis of pharmacological and therapeutic molecules.[58,59] Among them, imidazopyridine derivatives are significant pharmacophores that are present in many bio-

DOI: 10.1021/acs.inorgchem.7b00342
Inorg. Chem. XXXX, XXX, XXX−XXX

logically relevant compounds.[60] In particular, imidazo[1,2-*a*]pyridines exhibit promising biological properties.[61−66] In addition, the imidazo[1,2-*a*]pyridine core can be found in many natural products as well as in various pharmacological molecules such as anxyolytic drugs, viz., alpidem, necopidem, saripidem, and the drug that is useful in insomnia named zolpidem.[67] Naturally, great effort has been spent on their synthesis by using transition metal salts and other catalysts.[68−71] The synthesis of imidazopyridines is effected by using 2-aminopyiridine, an aldehyde, and a terminal alkyne through a one-pot three-component coupling reaction (TCC reaction, also known as A^3 coupling). First, it forms an intermediate propargylamine that further undergoes 5-exo-dig cyclization leading to the desired product (Table 1).[36] In our case, 10 wt % **LCu′** was added to the mixture containing 2-aminopyridine (1.1 mmol), benzaldehyde (1.2 mmol), and aryl alkynes (1 mmol) in toluene at 393 K under a N_2 atmosphere. The reaction of phenylacetylene with benzaldehyde and 2-aminopyridines gave the product in 89% yield (Table 1, entry 1). Aromatic alkynes having different substituents produced imidazopyridines in 73−86% yields. It was observed that aryl alkynes with electron-withdrawing groups gave yields higher than the yields of those having electron-donating groups (Table 1, entries 2−5). We performed another set of experiments in the absence of the catalyst that showed much smaller amounts of the desired product (Table 1, entry 7). Formation of the products was confirmed by ^{1}H and ^{13}C NMR and ESI mass spectroscopy (Figures S11−S25). The activity of **LCu′** was greatly superior to those of the homogeneous copper salts (Table 1, entry 6). Typically, upon completion of the reaction, the reaction mixture was filtered to separate the catalyst and washed several times with acetone, and after the mixture had been heated at 110 °C under vacuum, the active catalyst was regenerated. This regenerated catalyst was further used in the subsequent runs to check the recyclability. The catalytic activity of **LCu′** experienced only a slight degradation after three cycles (Figure S26). To better understand the framework integrity of the catalyst, PXRD measurement was conducted on the recovered catalyst after each cycle. No significant change observed in the PXRD pattern up to three cycles (Figure S27) demonstrated the maintenance of the framework integrity. The heterogeneous behavior of **LCu′** was unambiguously established by a hot filtration test (Figure S28).

LCu′-Catalyzed Pechmann Condensation: Synthesis of Coumarin Derivatives. In light of the importance of Pechmann condensation reactions in the synthesis of derivatives of coumarin, the heterogeneous catalytic activity of **LCu′** was further probed.

Coumarins are found to have varied biological activities[72−74] besides applications in food additives, fragrances, and cosmetics.[75] Coumarin derivatives can be synthesized by adopting various reactions.[76−81] The Pechmann reaction is the popular method that employs two-component coupling of phenol (2.1 mmol) and β-ketoester (2.5 mmol). To date, there have been several homogeneous, heterogeneous, and Lewis acid catalysts reported for this reaction.[82−86]

Herein, we showed the catalytic activity of **LCu′** in the Pechmann reaction using aromatic phenols with ethyl acetoacetate. As indicated in Table 2, a series of phenolic compounds were used to obtain the corresponding substituted coumarins. The results indicated that only 1,4-dihydroxynaphthalene, phenol, and 1-naphthol produced the product in average to good yields. The formation of the target products was confirmed using ^{1}H and ^{13}C NMR spectroscopy and ESI-MS analysis (Figures S29−S37), while the integrity of **LCu** after each catalytic run was evidenced by its PXRD pattern (Figure 3). In a similar way described by Cejka et al.,[84]

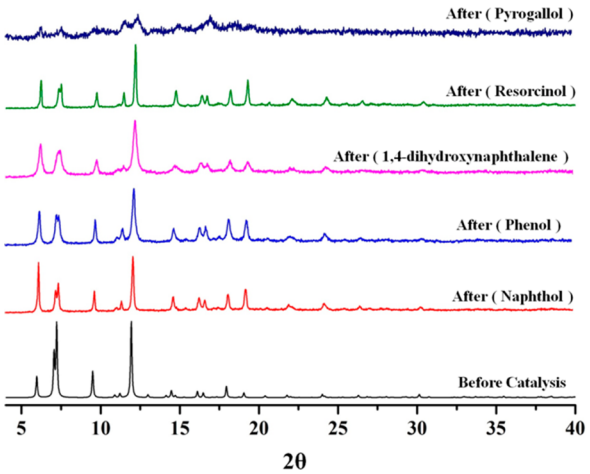

Figure 3. PXRD patterns of **LCu′** before and after the catalysis with different substrates.

negligible transformation of resorcinol and pyrogallol to the target coumarins was achieved using **LCu′** as a catalyst (Figures S38 and S39). In the case of resorcinol, the low catalytic activity of **LCu′** was assumed to be caused by its attachment to the UMCs of **LCu′**, thus blocking the reaction. In another case, the framework integrity collapsed in the presence of pyrogallol (Figure 3) under the reaction conditions. As mentioned above, here also the catalyst was recycled for two successive runs without any significant loss of activity (Figure S40). Catalyst **LCu′** preserved its integrity throughout the reaction as confirmed by PXRD (Figure S41). The heterogeneous behavior of **LCu′** was established by a hot filtration test (Figure S42).

■ CONCLUSION

In summary, we report here an enantiopure organic ligand, H_4L, incorporating the (*S*)-(+)-2-methylpiperazine moiety in its middle to construct the homochiral Cu(II) framework, **LCu**. The structure consists of $[Cu_2(COO)_4]$ paddle-wheel secondary bonding units (SBUs) with *NbO* topology. Interestingly, framework **LCu** exhibits excellent ferroelectric properties with an electric hysteresis loop showing a remnant polarization (P_r) of ∼3.5 μC cm^{-2} and a coercive field (E_c) of ∼12 kV cm^{-1}. Dielectric studies on **LCu** reveal almost frequency-independent behavior with a dielectric constant (ε_r) of ∼42 and a low dielectric loss (tan δ) of ∼0.04 up to 10^6, which suggests that it can be useful in high-frequency applications. Alternatively, activated framework **LCu′** exhibits efficient heterogeneous catalytic activity in the one-pot synthesis of imidazopyridine derivatives by the A^3 coupling reactions and synthesis of coumarin derivatives by the Pechmann reaction. Although the MOF is porous, we could not achieve adsorption of nitrogen gas. The causes for such behavior are being probed together with related samples that will constitute another study.

DOI: 10.1021/acs.inorgchem.7b00342
Inorg. Chem. XXXX, XXX, XXX−XXX

■ ASSOCIATED CONTENT

Supporting Information

The Supporting Information is available free of charge on the ACS Publications website at DOI: 10.1021/acs.inorgchem.7b00342.

Crystallographic data for **LCu** (CCDC 1531318) (CIF)
Several spectroscopic and thermogravimetric analyses, powder X-ray diffraction patterns, X-ray crystallographic data, and figures (PDF)

■ AUTHOR INFORMATION

Corresponding Author

*E-mail: pkb@iitk.ac.in.

ORCID

Rajesh Katoch: 0000-0003-2732-1309
Parimal K. Bharadwaj: 0000-0003-3347-8791

Notes

The authors declare no competing financial interest.

■ ACKNOWLEDGMENTS

We gratefully acknowledge the financial support received from the Department of Science and Technology, New Delhi, India (to R.K., A.G., and P.K.B.), and SRF from the CSIR to A.K.G. and D.D.

■ REFERENCES

(1) Zhou, H.-C.; Kitagawa, S. Metal−Organic Frameworks (MOFs). *Chem. Soc. Rev.* **2014**, *43*, 5415−5418.

(2) Li, J.-R.; Kuppler, R. J.; Zhou, H.-C. Selective gas adsorption and separation in metal−organic frameworks. *Chem. Soc. Rev.* **2009**, *38*, 1477−1504.

(3) De, D.; Pal, T. K.; Neogi, S.; Senthilkumar, S.; Das, D.; Gupta, S. S.; Bharadwaj, P. K. A Versatile CuII Metal−Organic Framework Exhibiting High Gas Storage Capacity with Selectivity for CO_2: Conversion of CO_2 to Cyclic Carbonate and Other Catalytic Abilities. *Chem. - Eur. J.* **2016**, *22*, 3387−3396.

(4) Liu, J.; Wang, F.; Ding, Q.-R.; Zhang, J. Synthesis of an Enantipure Tetrazole-Based Homochiral $Cu^{I,II}$-MOF for Enantioselective Separation. *Inorg. Chem.* **2016**, *55*, 12520−12522.

(5) Takashima, Y.; Martínez, V. M.; Furukawa, S.; Kondo, M.; Shimomura, S.; Uehara, H.; Nakahama, M.; Sugimoto, K.; Kitagawa, S. Molecular decoding using luminescence from an entangled porous framework. *Nat. Commun.* **2011**, *2*, 168.

(6) Sengupta, O.; Mukherjee, P. S. Mixed Azide and 5-(Pyrimidyl)-tetrazole Bridged Co(II)/Mn(II) Polymers: Synthesis, Crystal Structures, Ferroelectric and Magnetic Behavior. *Inorg. Chem.* **2010**, *49*, 8583−8590.

(7) Zeng, M.-H.; Yin, Z.; Tan, Y.-X.; Zhang, W.-X.; He, Y.-P.; Kurmoo, M. Nanoporous Cobalt(II) MOF Exhibiting Four Magnetic Ground States and Changes in Gas Sorption upon Post-Synthetic Modification. *J. Am. Chem. Soc.* **2014**, *136* (12), 4680−4688.

(8) Qiu, S.; Zhu, G. Molecular engineering for synthesizing novel structures of metal−organic frameworks with multifunctional properties. *Coord. Chem. Rev.* **2009**, *253*, 2891−2911.

(9) Debatin, F.; Thomas, A.; Kelling, A.; Hedin, N.; Bacsik, Z.; Senkovska, I.; Kaskel, S.; Junginger, M.; Müller, H.; Schilde, U.; Jäger, C.; Friedrich, A.; Holdt, H.-J. In Situ Synthesis of an Imidazolate-4-amide-5-imidate Ligand and Formation of a Microporous Zinc−Organic Framework with H2-and CO2-Storage Ability. *Angew. Chem., Int. Ed.* **2010**, *49*, 1258−1262.

(10) Ryu, D. W.; Lee, W. R.; Lim, K. S.; Phang, W. J.; Hong, C. S. Two Homochiral Bimetallic Metal−Organic Frameworks Composed of a Paramagnetic Metalloligand and Chiral Camphorates: Multifunctional Properties of Sorption, Magnetism, and Enantioselective Separation. *Cryst. Growth Des.* **2014**, *14*, 6472−6477.

(11) Karmakar, A.; Desai, A. V.; Manna, B.; Joarder, B.; Ghosh, S. K. An Amide-Functionalized Dynamic Metal−Organic Framework Exhibiting Visual Colorimetric Anion Exchange and Selective Uptake of Benzene over Cyclohexane. *Chem. - Eur. J.* **2015**, *21*, 7071−7076.

(12) Vanderah, T. A. Talking Ceramics. *Science* **2002**, *298*, 1182−1184.

(13) Horiuchi, S.; Tokura, Y. Organic ferroelectrics. *Nat. Mater.* **2008**, *7*, 357−366.

(14) Rogez, G.; Viart, N.; Drillon, M. Multiferroic Materials: The Attractive Approach of Metal−Organic Frameworks (MOFs). *Angew. Chem., Int. Ed.* **2010**, *49*, 1921−1923.

(15) Scott, J. F. Applications of Modern Ferroelectrics. *Science* **2007**, *315*, 954−959.

(16) Rijnders, G.; Blank, D. H. A. Materials science: Build your own superlattice. *Nature* **2005**, *433*, 369−370.

(17) Lee, H. N.; Christen, H. M.; Chisholm, M. F.; Rouleau, C. M.; Lowndes, D. H. Strong polarization enhancement in asymmetric three-component ferroelectric superlattices. *Nature* **2005**, *433*, 395−399.

(18) Yan, H.; Zhang, H.; Ubic, R.; Reece, M. J.; Liu, J.; Shen, Z.; Zhang, Z. A Lead-Free High-Curie-Point Ferroelectric Ceramic, $CaBi_2Nb_2O_9$. *Adv. Mater.* **2005**, *17*, 1261−1265.

(19) Zhang, W.; Xiong, R.-G.; Huang, S. D. 3D framework containing Cu4Br4 cubane as connecting node with strong ferroelectricity. *J. Am. Chem. Soc.* **2008**, *130*, 10468−10469.

(20) Zhao, H.; Qu, Z.-R.; Ye, H.-Y.; Xiong, R.-G. In situ hydrothermal synthesis of tetrazole coordination polymers with interesting physical properties. *Chem. Soc. Rev.* **2008**, *37*, 84−100.

(21) Ye, Q.; Song, Y.-M.; Fu, D.-W.; Wang, G.-X.; Xiong, R.-G.; Chan, P. W. H.; Huang, S. D. Deuteration effect of ferroelectricity and permittivity on homochiral zinc coordination compound. *Cryst. Growth Des.* **2007**, *7*, 1568−1570.

(22) Gu, Z.-G.; Zhou, X.-H.; Jin, Y.-B.; Xiong, R.-G.; Zuo, J.-L.; You, X.-Z. Crystal Structures and Magnetic and Ferroelectric Properties of Chiral Layered Metal−Organic Frameworks with Dicyanamide as the Bridging Ligand. *Inorg. Chem.* **2007**, *46*, 5462−5464.

(23) Zhang, W.; Ye, H.-Y.; Xiong, R.-G. Metal-organic coordination compounds for potential ferroelectrics. *Coord. Chem. Rev.* **2009**, *253*, 2980−2997.

(24) Halasyamani, P. S.; Poeppelmeier, K. R. Noncentrosymmetric oxide. *Chem. Mater.* **1998**, *10*, 2753−2769.

(25) The corresponding 10 point group symmetries are given in parentheses after the crystal classes: 1 (*C*1), m (*Cs*), 2 (*C*2), mm2 (*C*2*v*), 3 (*C*3), 3m (*C*3*v*), 4 (*C*4), 4mm (*C*4*v*), 6 (*C*6), and 6mm (*C*6*v*).

(26) Ahmad, M.; Katoch, R.; Garg, A.; Bharadwaj, P. K. A novel 3D 10-fold interpenetrated homochiral coordination polymer: large spontaneous polarization, dielectric loss and emission studies. *CrystEngComm* **2014**, *16*, 4766−4773.

(27) Pal, T. K.; De, D.; Senthilkumar, S.; Neogi, S.; Bharadwaj, P. K. A Partially Fluorinated, Water-Stable Cu(II)−MOF Derived via Transmetalation: Significant Gas Adsorption with High CO2 Selectivity and Catalysis of Biginelli Reactions. *Inorg. Chem.* **2016**, *55*, 7835−7842.

(28) Shi, L.-X.; Wu, C.-D. A nanoporous metal−organic framework with accessible Cu^{2+} sites for the catalytic Henry reaction. *Chem. Commun.* **2011**, *47*, 2928−2930.

(29) Shi, L.-X.; Wu, C.-D. A nanoporous metal−organic framework with accessible Cu2+ sites for the catalytic Henry reaction. *Chem. Commun.* **2011**, *47*, 2928−2930.

(30) Gu, Z.-Y.; Park, J.; Raiff, A.; Wei, Z.; Zhou, H.-C. Metal−organic frameworks as biomimetic catalysts. *ChemCatChem* **2014**, *6*, 67−75.

(31) Valvekens, P.; Vermoortele, F.; De Vos, D. Metal−organic frameworks as catalysts: the role of metal active sites. *Catal. Sci. Technol.* **2013**, *3*, 1435−1445.

(32) Liu, J.; Chen, L.; Cui, H.; Zhang, J.; Zhang, L.; Su, C.-Y. Applications of metal−organic frameworks in heterogeneous supramolecular catalysis. *Chem. Soc. Rev.* **2014**, *43*, 6011−6061.

(33) Valvekens, P.; Vandichel, M.; Waroquier, M.; Van Speybroeck, V.; De Vos, D. Metal-dioxidoterephthalate MOFs of the MOF-74

DOI: 10.1021/acs.inorgchem.7b00342
Inorg. Chem. XXXX, XXX, XXX−XXX

type: Microporous basic catalysts with well-defined active sites. *J. Catal.* **2014**, *317*, 1−10.
(34) Phan, N. T. S.; Vu, P. H. L.; Nguyen, T. T. Expanding applications of copper-based metal−organic frameworks in catalysis: Oxidative C−O coupling by direct C−H activation of ethers over $Cu_2(BPDC)_2(BPY)$ as an efficient heterogeneous catalyst. *J. Catal.* **2013**, *306*, 38−46.
(35) Dhakshinamoorthy, A.; Alvaro, M.; Garcia, H. Metal-Organic Frameworks (MOFs) as Heterogeneous Catalysts for the Chemoselective Reduction of Carbon-Carbon Multiple Bonds with Hydrazine. *Adv. Synth. Catal.* **2009**, *351*, 2271−2276.
(36) Luz, I.; Llabrés i Xamena, F. X.; Corma, A. Bridging homogeneous and heterogeneous catalysis with MOFs: Cu-MOFs as solid catalysts for three-component coupling and cyclization reactions for the synthesis of propargylamines, indoles and imidazopyridines. *J. Catal.* **2012**, *285*, 285−291.
(37) Ruano, D.; Díaz-García, M.; Alfayate, A.; Sánchez-Sánchez, M. Nanocrystalline M−MOF-74 as Heterogeneous Catalysts in the Oxidation of Cyclohexene: Correlation of the Activity and Redox Potential. *ChemCatChem* **2015**, *7*, 674−681.
(38) He, Y.; Li, B.; O'Keeffe, M.; Chen, B. Multifunctional metal−organic frameworks constructed from meta-benzenedicarboxylate units. *Chem. Soc. Rev.* **2014**, *43*, 5618−5656.
(39) Willis, M. C.; Chauhan, J.; Whittingham, W. G. A new reactivity pattern for vinyl bromides: cine-substitution via palladium catalysed C−N coupling/Michael addition reactions. *Org. Biomol. Chem.* **2005**, *3*, 3094−3095.
(40) Lin, X.; Telepeni, I.; Blake, A. J.; Dailly, A.; Brown, C. M.; Simmons, J. M.; Zoppi, M.; Walker, G. S.; Thomas, K. M.; Mays, T. J.; Hubberstey, P.; Champness, N. R.; Schröder, M. High capacity hydrogen adsorption in Cu (II) tetracarboxylate framework materials: the role of pore size, ligand functionalization, and exposed metal sites. *J. Am. Chem. Soc.* **2009**, *131*, 2159−2171.
(41) Lu, W.; Yuan, D.; Makal, T. A.; Li, J.-R.; Zhou, H.-C. A Highly Porous and Robust (3,3,4)-Connected Metal−Organic Framework Assembled with a 90° Bridging-Angle Embedded Octacarboxylate Ligand. *Angew. Chem., Int. Ed.* **2012**, *51*, 1580−1584; *Angew. Chem.* **2012**, *124*, 1612−1616.
(42) Pan, L.; Liu, G.; Li, H.; Meng, S.; Han, L.; Shang, J.; Chen, B.; Platero-Prats, A. E.; Lu, W.; Zou, X.; Li, R.-W. A Resistance-Switchable and Ferroelectric Metal−Organic Framework. *J. Am. Chem. Soc.* **2014**, *136*, 17477−17483.
(43) Thomson, R. I.; Jain, P.; Cheetham, A. K.; Carpenter, M. A. Elastic relaxation behavior, magnetoelastic coupling, and order-disorder processes in multiferroic metal-organic frameworks. *Phys. Rev. B: Condens. Matter Mater. Phys.* **2012**, *86*, 214304.
(44) Tian, Y.; Stroppa, A.; Chai, Y.; Yan, L.; Wang, S.; Barone, P.; Picozzi, S.; Sun, Y. Cross coupling between electric and magnetic orders in a multiferroic metal-organic framework. *Sci. Rep.* **2014**, *4*, 6062.
(45) Yang, J.; Zhou, L.; Cheng, J.; Hu, Z.; Kuo, C.; Pao, C.-W.; Jang, L.; Lee, J.-F.; Dai, J.; Zhang, S.; Feng, S.; Kong, P.; Yuan, Z.; Yuan, J.; Uwatoko, Y.; Liu, T.; Jin, C.; Long, Y. Charge Transfer Induced Multifunctional Transitions with Sensitive Pressure Manipulation in a Metal−Organic Framework. *Inorg. Chem.* **2015**, *54*, 6433−6438.
(46) Tian, Y.; Shen, S.; Cong, J.; Yan, L.; Wang, S.; Sun, Y. Observation of Resonant Quantum Magnetoelectric Effect in a Multiferroic Metal−Organic Framework. *J. Am. Chem. Soc.* **2016**, *138*, 782−785.
(47) Yadav, R.; Swain, D.; Bhat, H. L.; Elizabeth, S. Order-disorder phase transition and multiferroic behaviour in a metal organic framework compound $(CH_3)_2NH_2Co(HCOO)_3$. *J. Appl. Phys.* **2016**, *119*, 064103.
(48) Holden, A. N.; Matthias, B. T.; Merz, W. J.; Remeika, J. P. New Class of Ferroelectrics. *Phys. Rev.* **1955**, *98*, 546.
(49) Schein, B. J. B.; Lingafelter, E. C.; Stewart, J. M. Redetermination of the Structure of the Ferroelectric Crystal Guanidinium Aluminum Sulfate Hexahydrate, GASH, and its Chromium Isomorph. *J. Chem. Phys.* **1967**, *47*, 5183.
(50) Jakubas, R.; Czapla, Z.; Galewski, Z.; Sobczyk, L. Ferroelectric phase transition in $[(CH_3)_3\ NH]_3\ Sb_2Cl_9$ (TMACA). *Ferroelectr., Lett. Sect.* **1986**, *5*, 143−148.
(51) Jakubas, R. A new ferroelectric compound:$(CH_3NH_3)_5Bi_2Br_{11}$. *Solid State Commun.* **1989**, *69*, 267−269.
(52) Tang, Y.-Z.; Zhou, M.; Huang, J.; Tan, Y.-H.; Wu, J.-S.; Wen, H.-R. In situ synthesis and ferroelectric, SHG response, and luminescent properties of a novel 3D acentric zinc coordination polymer. *Inorg. Chem.* **2013**, *52*, 1679−1681.
(53) Zhang, C.; Chi, Q.; Dong, J.; Cui, Y.; Wang, X.; Liu, L.; Lei, Q. Enhanced dielectric properties of poly (vinylidene fluoride) composites filled with nano iron oxide-deposited barium titanate hybrid particles. *Sci. Rep.* **2016**, *6*, 33508.
(54) Fu, J.; Hou, Y.; Zheng, M.; Wei, Q.; Zhu, M.; Yan, H. Improving dielectric properties of PVDF composites by employing surface modified strong polarized BaTiO3 particles derived by molten salt method. *ACS Appl. Mater. Interfaces* **2015**, *7*, 24480−24491.
(55) Thirmal, C.; Nayek, C.; Murugavel, P.; Subramanian, V. Magnetic, dielectric and magnetodielectric properties of PVDF-$La_{0.7}Sr_{0.3}MnO_3$ polymer nanocomposite film. *AIP Adv.* **2013**, *3*, 112109.
(56) Yang, J.; Pan, P.; Hua, L.; Feng, X.; Yue, J.; Ge, Y.; Inoue, Y. Effects of Crystallization Temperature of Poly(vinylidene fluoride) on Crystal Modification and Phase Transition of Poly(butylene adipate) in Their Blends: A Novel Approach for Polymorphic Control. *J. Phys. Chem. B* **2012**, *116*, 1265−1272.
(57) Yu, K.; Wang, H.; Zhou, Y.; Bai, Y.; Niu, Y. Enhanced dielectric properties of BaTiO3/poly (vinylidene fluoride) nanocomposites for energy storage applications. *J. Appl. Phys.* **2013**, *113*, 034105.
(58) Butler, M. S. The role of natural product chemistry in drug discovery. *J. Nat. Prod.* **2004**, *67*, 2141−2153.
(59) Joule, J. A.; Mills, K. *Heterocyclic Chemistry*; Blackwell Science: Oxford, U.K., 2000.
(60) Couty, F.; Evano, G. In *Comprehensive Heterocyclic Chemistry III*; Katritzky, A. R., Ramsden, C. A., Scriven, E. F. V., Taylor, R. J. K., Eds.; Elsevier: Oxford, U.K., 2008; Vol. 11, pp 409−499, and references therein.
(61) Anaflous, A.; Benchat, N.; Mimouni, M.; Abouricha, S.; Ben-Hadda, T.; El-Bali, B.; Hakkou, A.; Hacht, B. Armed imidazo[1,2-*a*]pyridines (pyridines): evaluation of antibacterial activity. *Lett. Drug Des. Discovery* **2004**, *1*, 224−229.
(62) Lhassani, M.; Chavignon, O.; Chezal, J.-M.; Teulade, J.-C.; Chapat, J.-P.; Snoeck, R.; Andrei, G.; Balzarini, J.; De Clercq, E.; Gueiffier, A. Synthesis and antiviral activity of imidazo[1,2-*a*]pyridines. *Eur. J. Med. Chem.* **1999**, *34*, 271−274.
(63) Rupert, K. C.; Henry, J. R.; Dodd, J. H.; Wadsworth, S. A.; Cavender, D. E.; Olini, G. C.; Fahmy, B.; Siekierka, J. Imidazopyrimidines, potent inhibitors of p38 MAP kinase. *Bioorg. Med. Chem. Lett.* **2003**, *13*, 347−350.
(64) Meirer, K.; Rödl, C. B.; Wisniewska, J. M.; George, S.; Häfner, A. K.; Buscató, E.; Klingler, F. M.; Hahn, S.; Berressem, D.; Wittmann, S. K.; Steinhilber, D.; Hofmann, B.; Proschak, E. Synthesis and Structure−Activity Relationship Studies of Novel Dual Inhibitors of Soluble Epoxide Hydrolase and 5-Lipoxygenase. *J. Med. Chem.* **2013**, *56*, 1777−1781.
(65) Enguehard-Gueiffier, C.; Musiu, S.; Henry, N.; Véron, J. B.; Mavel, S.; Neyts, J.; Leyssen, P.; Paeshuyse, J.; Gueiffier, A. 3-Biphenylimidazo [1,2-*a*] pyridines or [1, 2-*β*] pyridazines and analogues, novel Flaviviridae inhibitors. *Eur. J. Med. Chem.* **2013**, *64*, 448−463.
(66) Ulloora, S.; Shabaraya, R.; Aamir, S.; Adhikari, A. V. New imidazo [1,2-*a*] pyridines carrying active pharmacophores: Synthesis and anticonvulsant studies. *Bioorg. Med. Chem. Lett.* **2013**, *23*, 1502−1506.
(67) Enguehard-Gueiffier, C.; Gueiffier, A. Recent progress in the pharmacology of imidazo [1,2-*a*] pyridines. *Mini-Rev. Med. Chem.* **2007**, *7*, 888−899.

DOI: 10.1021/acs.inorgchem.7b00342
Inorg. Chem. XXXX, XXX, XXX−XXX

(68) Liu, P.; Fang, L.-S.; Lei, X.; Lin, G.-Q. Synthesis of imidazo [1,2-*a*] pyridines via three-component reaction of 2-aminopyridines, aldehydes and alkynes. *Tetrahedron Lett.* **2010**, *51*, 4605−4608.
(69) Chernyak, N.; Gevorgyan, V. General and Efficient Copper-Catalyzed Three-Component Coupling Reaction towards Imidazoheterocycles: One-Pot Synthesis of Alpidem and Zolpidem. *Angew. Chem., Int. Ed.* **2010**, *49*, 2743−2746.
(70) Yadav, J. S.; Subba Reddy, B. V.; Gopal Rao, Y.; Srinivas, M.; Narsaiah, A. V. Cu (OTf) 2-catalyzed synthesis of imidazo [1, 2-*a*] pyridines from α-diazoketones and 2-aminopyridines. *Tetrahedron Lett.* **2007**, *48*, 7717−7720.
(71) Bakherad, M.; Nasr-Isfahani, H.; Keivanloo, A.; Doostmohammadi, N. Pd−Cu catalyzed heterocyclization during Sonogashira coupling: synthesis of 2-benzylimidazo [1, 2-*a*] pyridine. *Tetrahedron Lett.* **2008**, *49*, 3819−3822.
(72) Ahadi, S.; Zolghadr, M.; Khavasi, H. R.; Bazgir, A. A diastereoselective synthesis of pyrano fused coumarins via organocatalytic three-component reaction. *Org. Biomol. Chem.* **2013**, *11*, 279−286.
(73) Nofal, Z. M.; El-Masry, H.; Fahmy, H. H.; Sarhan, Al. Synthesis of some new coumarin derivatives incorporated to heterocyclic aromatic rings. *Egypt. J. Pharm. Sci.* **1997**, *38*, 1−11.
(74) Nofal, Z. M.; El-Zahar, M. I.; Abd-El-Karim, S. S. Novel coumarin derivatives with expected biological activity. *Molecules* **2000**, *5*, 99−113.
(75) Romanelli, G. P.; Bennardi, D.; Ruiz, D. M.; Baronetti, G.; Thomas, H. J.; Autino, J. C. A solvent-free synthesis of coumarins using a Wells−Dawson heteropolyacid as catalyst. *Tetrahedron Lett.* **2004**, *45*, 8935−8939.
(76) Von Pechmann, H.; Duisberg, C. *Ber. Dtsch. Chem. Ges.* **1884**, *17*, 929−936.
(77) Johnson, J. R. The Perkin reaction and related reactions. *Org. React.* **1942**, *1*, 210−265.
(78) Brufola, G.; Fringuelli, F.; Piermatti, O.; Pizzo, F. Simple and Efficient One-Pot Preparation of 3-Substituted Coumarins in Water. *Heterocycles* **1996**, *43*, 1257−1266.
(79) Shirner, R. L. The reformatsky reaction. *Org. React.* **1942**, *1*, 1−37.
(80) Yavari, I.; Hekmat-Shoar, R.; Zonouzi, A. A new and efficient route to 4-carboxymethylcoumarins mediated by vinyltriphenylphosphonium salt. *Tetrahedron Lett.* **1998**, *39*, 2391−2392.
(81) Cartwright, G. A.; McNab, W. Synthesis of Coumarins by Flash Vacuum Pyrolysis of 3-(2-Hydroxyaryl)propenoic Esters. *J. Chem. Res., Synop.* **1997**, 296−297.
(82) Canter, F. W.; Curd, F. H.; Robertson, A. CLXV. -Hydroxycarbonyl Compounds. Part II. The Benxoylation of Ketones derived from Phloroglucinol. *J. Chem. Soc.* **1931**, *0*, 1245−1255.
(83) Woods, L. L.; Sapp, J. A New One-Step Synthesis of Substituted Coumarins. *J. Org. Chem.* **1962**, *27*, 3703−3705.
(84) Opanasenko, M.; Shamzhy, M.; Cejka, J. Solid acid catalysts for coumarin synthesis by the Pechmann reaction: MOFs versus zeolites. *ChemCatChem* **2013**, *5*, 1024−1031.
(85) Niharika, P.; Ramulu, B. V.; Satyanarayana, G. Lewis acid promoted dual bond formation: facile synthesis of dihydrocoumarins and spiro-tetracyclic dihydrocoumarins. *Org. Biomol. Chem.* **2014**, *12*, 4347−4360.
(86) Valizadeh, H.; Shockravi, A. An efficient procedure for the synthesis of coumarin derivatives using TiCl 4 as catalyst under solvent-free conditions. *Tetrahedron Lett.* **2005**, *46*, 3501−3503.

DOI: 10.1021/acs.inorgchem.7b00342
Inorg. Chem. XXXX, XXX, XXX−XXX